Spectral Overlap of Saliency Signal Components in Injection Based Sensorless Controlled Induction Machines

T. M. Wolbank
Member
Department of Electrical Drives and Machines
Vienna University of Technology
Vienna, Austria
e-mail: thomas.wolbank@tuwien.ac.at

M. K. Metwally
Department of Electrical Engineering, Faculty of Engineering, Menoufia University
Menoufia, Egypt

***Abstract*— Sensorless control techniques of ac machines based on fundamental wave methods have a critical point of operation at zero frequency. Using signal injection methods zero frequency operation is possible, however another critical point of operation may exist at overlap frequencies which, so far has not been addressed by research. The resulting signals from injection based sensorless control methods are composed of components caused by saturation, slotting or anisotropy saliencies, as well as inter-modulation effects. The point of operation where the frequency of the slotting saliency equals the frequency of the saturation saliency is critical in terms of control performance as then a reliable separation is only possible feed forward. A mathematical description of the relation between the mechanical speed and load torque at the overlap of the slotting and saturation frequencies is given. Measurement results at specific points of operation are shown to point out that the critical point of operation is no longer zero speed or zero frequency but may be one of the operating states where an overlap in frequencies exists.**

Index Terms — Pulse injection; Saturation saliency; Slotting saliency; Inter-modulation induced signal; Fourier transform; Induction machine.

I. Introduction

High dynamic control of induction machines is only achievable by some sort of field oriented control. Realizing this type of control without using a shaft sensor has the advantage of increased reliability and decreased costs. Although used in the higher frequency range, methods considering only fundamental wave quantities of the machine will deteriorate in their performance at low or zero stator frequency due to the lack of signal and an increasing influence of noise and parameter uncertainties [1].

For all applications that need controlled operation at zero speed, the only solution so far is to exploit non-fundamental effects of the machine. These non-fundamental or parasitic effects can be either engineered saliencies, or inherent saliencies, like the asymmetry caused by spatial flux saturation, or the slotting of the machine.

All of these effects lead to a modulation of the transient machine reactance that depends on the position of the corresponding asymmetry. The resulting modulation of the transient reactance can be estimated by an excitation of the machine with voltage pulses or a high frequency carrier signal in addition to the fundamental wave. Using appropriate evaluation algorithms it is thus possible to estimate the flux and/or rotor position even at zero speed without requiring a shaft sensor. According to the necessary excitation of the machine the methods based on the detection of parasitic effects are usually called signal injection methods.

The excitation can be either a transient signal by using the voltage pulses generated by the switching of the voltage source inverter and by exploiting the resulting transient current change as proposed in [2], [3]. Alternatively it is also possible to impress a balanced poly phase voltage signal in addition to the fundamental wave as proposed for example in [4], [7].

In recent years several new signal injection based approaches that integrate the *di/dt* measurements within the fundamental space vector PWM (SVPWM) sequence have been presented [8]-[11]. They all use the inverter states of a PWM cycle (either only the active or the active plus the inactive state) to exploit the saliency information. To avoid the parasitic effects of the non ideal inverter especially near zero frequency, only the two active states are used in [12]. The method applied in the following evaluates the transient current change resulting from active voltage pulse excitation, which is mainly affected by the flux/load dependence [2].

Another point that has to be taken into account is that the saliency information of the flux (saturation dependent) is superposed with all other saliencies present in an induction machine, as there are rotor anisotropy, and slotting. It is obvious that there exist specific operating conditions where for example the frequency of the saturation signal equals that of the main slotting signal (fundamental frequency times number of pole pairs = mechanical speed times number of rotor slots). In these cases a separation of the two components is not possible in practical operation using filters or frequency based approaches. Research has up to now concentrated on zero speed, so these operating ranges have not been addressed in literature so far.

The following investigation will focus on presenting a mathematical description of the relationship between the mechanical speed and load torque at the different possible overlap situations of the slotting and saturation frequencies in the positive and negative speed operation.

All measurement results presented are based on a standard induction machine with unskewed open rotor slots. They are however, also applicable to all multi-saliency machines. Measurement results at different specific points of operation are shown to point out that the critical point of operation is no

978-1-4244-5287-3/10/$26.00 ©2010 IEEE

longer zero speed or zero frequency but one of the operating states where an overlap in frequencies exists.

II. Voltage Pulse Excitation

The necessary transient excitation for these measurements and the resulting signal processing was done based on the sensorless control scheme, named INFORM ("Indirect Flux detection by Online Reactance Measurement") [2].

It uses a transient excitation of the machine with voltage pulses imposed by the inverter and evaluates the change of the machines line currents due to these pulses. The reaction of the machine is measured as the current slope for each single phase. This transient current slope of an induction machine is determined by the stator equation of the machine as in (1).

$$\underline{u}_S = r_S \cdot \underline{i}_S + l_\sigma \cdot \frac{d\,\underline{i}_S}{dt} + \underline{emf} \tag{1}$$

The transient change in the machine current $d\underline{i}_s/dt$ is thus determined by the voltage $\underline{u}_s$ applied, whose magnitude is proportional to the dc link voltage during an active inverter switching state, as well as by the value of the leakage inductance l_σ. Additional influences are the stator resistance voltage drop $r_s \cdot \underline{i}_s$ and the back electromotive force emf. The mentioned inherent saliencies have almost negligible influence on the fundamental wave behavior of the machine.

They mainly affect only the transient leakage inductance and by measuring the transient current response it is thus possible to detect and locate their positions. As the contribution of the transient reactance on the overall transient current change decreases, especially when compared to the back emf from some percent of the rated speed onward, all other influences act as disturbance and have to be eliminated.

The influence of stator resistance voltage drop $r_s \cdot \underline{i}_s$ and back emf have to be eliminated by evaluating the current change of two subsequent active voltage phasors pointing in different spatial directions. This is the main reason why a pulse sequence of at least two pulses is usually applied as excitation signal. The signal obtained after applying the algorithm consists of a mean value, according to the mean transient reactance, and of modulations caused by the rotation of the individual saliencies.

If the excitation is realized in all three stator phases, the tip of the resulting current change space phasor (evaluated for a given set of two active voltage phasors) describes a circle for each set of voltage phasors. Each circle has an offset in the direction of the corresponding phase. This offset represents the mean value of the transient reactance, which is a measure of the total saturation level in the machine. The offset can be eliminated feed forward and the resulting signal now gives the modulation of the transient reactances with the saliencies and thus contains information about the flux and rotor angular position.

The most prominent modulation is caused by saturation of the iron core due to the fundamental wave and has a period of two cycles per pole pair. Because of its relatively high magnitude it is often exploited in sensorless control schemes to detect the flux position. Another saliency is caused by the distribution of the stator and rotor winding in slots. Especially under loaded conditions it is much less prominent than the saturation saliency. This often is a limit for a position detection using this saliency. The main problem in the realization of sensorless control schemes is the interaction of these main modulations. They can only be separated by advanced observers or filtering techniques if their frequencies clearly differ from each other. However, there are specific points of operation where the signals of both saliencies have the same frequency and superpose each other. Besides a robust signal processing method to separate these signal components, it is thus desirable for practical operation to influence the saliencies by a suitable design of the machine. Thus only one prominent modulation can be enlarged by suppressing the others.

III. Mathematical Description

The relation between the slip frequency, the electrical and mechanical frequency can be written as in (2).

$$\omega_{slip} = \omega_{el} - \omega_m \cdot pp \tag{2}$$

Where ω_{slip} is the slip, and ω_{el} is the electrical frequency, ω_m is the mechanical rotor frequency, and pp is number of pole pairs.

The slotting frequency obtained from the slotting saliency equals the mechanical frequency times the number of rotor slots as in (3).

$$\omega_{slot} = n_R . \omega_m \tag{3}$$

Where ω_{slot} is the slot frequency, and n_R is the number of rotor slots. Substituting from (3) in (2) leads to

$$\omega_{slip} = \omega_{el} - \frac{\omega_{slot}}{n_R} pp\ . \tag{4}$$

From (4) the slotting frequency in the positive and negative rotating directions can be expressed as a relation of the slip, and electrical frequencies as in (5).

$$\omega_{slot} = \pm n_R \frac{(\omega_{el} - \omega_{slip})}{pp} \tag{5}$$

The saturation frequency ω_{sat} obtained from the saturation saliency is linked to the electrical frequency by a factor 2 as only saturation level not its direction is detected (6).

$$\omega_{sat} = 2 . \omega_{el} \tag{6}$$

The incidence of a frequency component overlap, where the saturation frequency equals the slotting frequency occurs when the condition expressed in (7) is met.

$$2 . \omega_{el} = \pm n_R \frac{(\omega_{el} - \omega_{slip})}{pp} \tag{7}$$

The ± sign in (7) indicates overlap situations occurring when the saturation and slotting frequency are of same magnitude and direction as well as of same magnitude and opposite direction. Both of these situations are critical in terms of sensorless control performance.

Slip frequency in induction machines is a linear function of flux and torque. With the data of the machine under test (44 rotor slots, 36 stator slots, 4 poles) the relationship between the slip and torque T under rated flux level can be written as in (8).

$$\omega_{slip} = \left|K\right|.T \tag{8}$$

Where the constant K defines the slip frequency at rated torque. By the substitution of (8) into (7) the electrical speed at the frequency overlap condition is obtained. Using (2) the corresponding mechanical speed can finally be calculated.

For each torque value two overlap conditions exist, one where both, slotting frequency and saturation frequency have the same sign and another where one of the two frequencies is negative.

When scaling the frequencies in revolutions per minute the proportional factor K for the machine considered in this investigations is identified to 52.6. The corresponding mechanical speeds when the slotting saliency frequency equals the saturation saliency frequency can then be calculated as given in (9) and (10) respectively as a function of load torque.

$$\omega_m = 2.63 \cdot T \tag{9}$$

The constant 2.63 (9) is obtained for frequency overlap and equal direction of rotation of the two saliencies and the constant -2.19 (10) for opposite direction of rotation.

$$\omega_m = -2.19 \cdot T \tag{10}$$

Except for these two operating conditions the frequencies of the slotting and saturation saliencies will not be the same.

In addition to the saturation component, the interaction between the saturation and the rotor-stator slotting harmonic will give rise to the inter-modulation (IM) component with a considerable magnitude in the resulting saliency control signal. This signal component leads to additional possible spectral overlap situations of now three signal components.

The relation between the harmonic orders of the inter-modulation induced component, the slotting, and saturation saliencies is given in (11). The magnitude of the inter-modulation induced disturbance is load dependent.

$$H_{int} = (\pm1)\cdot H_{slot} + (\pm1)\cdot H_{sat} \tag{11}$$

Where H_{int} is the inter-modulation harmonic order, H_{slot} is the slotting harmonic order, and H_{sat} is the saturation harmonic order. The negative sign is used for machines where the number of rotor slots is greater than number of stator slots and the positive sign is used when the number of rotor slots less than number of stator slots.

The conditions where the harmonics of the intermodulation signal superposes with one of the main saliencies are thus given by (12).

$$2H_{sat}=-H_{slot} \quad \text{and} \quad 2H_{slot}=-H_{sat} \tag{12}$$

IV. Experimental Results

The experimental results shown are obtained from an induction machine drive with 44 un-skewed, open rotor slots, and 36 stator slots coupled to a speed controlled load machine. The machine under test was operated under sensor field oriented torque controlled conditions. The parameters of the induction motor are given in appendix I.

The control is done on a digital signal processor board plugged into a computer. It performs the vector control. The pulse sequences and instances of injections are being calculated on a field programmable gate array system (FPGA) plugged into another computer. There is a communication board between the two systems for transferring and receiving data. The induction motor was fed by a voltage source inverter with PWM (5 kHz). Three industrial current sensors were used for the current measurements. The position signal is available from an encoder with 1024 pulses resolution.

In the following all FFT spectra are analyzed with respect to one electrical revolution.

In a first test the machine was operated at zero load to show the signal components of the different saliencies that are all contained in the measured modulation of the transient leakage inductance.

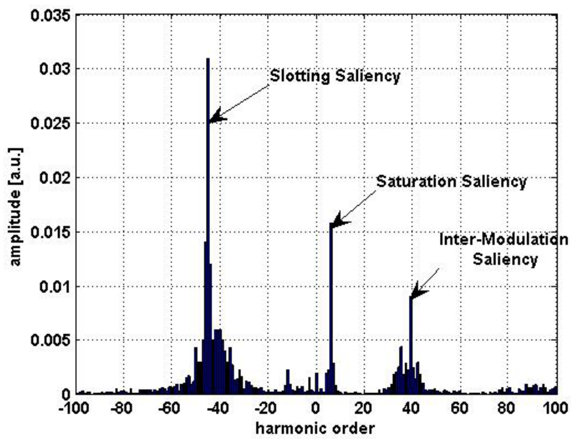

Fig. 1: Spectral components of machine at no load condition.

The resulting modulation contains three clearly distinguishable signal components corresponding to the main saliency components. The fundamental frequency of the FFT in this figure equals one mechanical period thus the saturation saliency is visible as $+4^{th}$ harmonic in the spectrum. Due to the no load condition and the machine construction (number of rotor slots equal 44, stator slots 36, pole pair number 2) the slotting component results in a -44^{th} harmonic. Finally the intermodulation component between saturation and slotting is obtained according to (11) as $+40^{th}$ harmonic. In this operating range a clear separation of each signal component is possible without reducing control performance.

Situation changes when the machine is loaded. In Fig. 2 (upper diagram) the FFT spectrum of the resulting saliency signal at 92% rated load and the machine rotating at a speed of 2.42 rpm is depicted. As shown in the figure, at this point of operation the slotting modulation (Slotting) depicted as -2nd harmonic is rotating with the same angular speed, but with opposite direction as the saturation modulation (Saturation) (depicted as +2nd harmonic). The harmonic component caused by the interaction of saturation and slotting signals, as described above, in this case is visible as offset component according to (11).

Fig. 2 (lower diagram) shows the locus of the real and imaginary components of the resulting saliency control signals which is visible as a line with an offset from the zero point due to inter-modulation effect. It is obvious that estimating the flux or rotor angle is quite challenging in this point of operation if the separation of the different components is not accurately performed by feed forward measures.

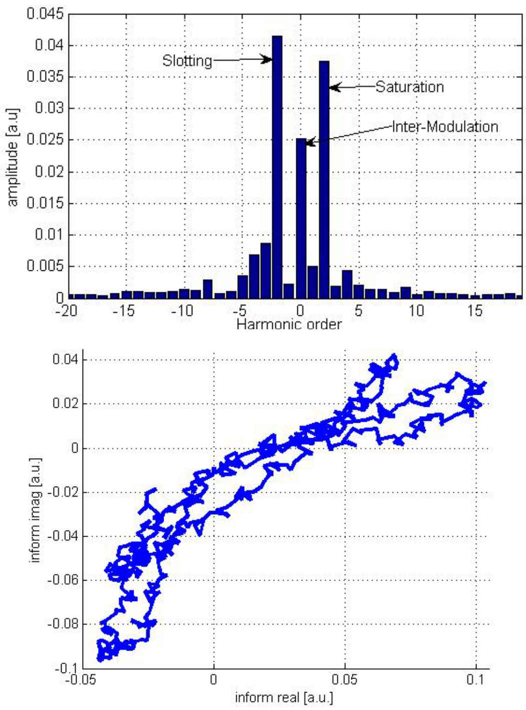

Fig. 2: Overlap of saliency signal components at 92% rated load and 2.42 rpm. Upper: FFT spectrum; Lower: XY plot of real and imaginary parts of saliency control signals.

When leaving the load current from Fig. 2 unchanged changing only slightly the mechanical speed another overlap situation occurs. This is depicted in Fig. 3. The upper diagram shows the FFT spectrum of the resulting saliency signal at 92% rated load and the machine rotating at a speed of -2.024 rpm.

As shown in the figure at this point of operation the slotting modulation has as harmonic order of +2. It is rotating with the same angular speed and in the same direction as the saturation modulation (also +2nd harmonic). The harmonic component caused by the interaction of saturation and slotting modulation as described in (11) is now the -4th harmonic rotating in the opposite direction. Fig. 2 (lower diagram) shows the locus of the real and imaginary components of the resulting saliency control signals, which is depicted as a triangle. Again it can be seen that also in this point of operation is critical in terms of extraction of flux/rotor position. To avoid deterioration of the control performance it is quite important to have a very accurate feed forward separation of the components.

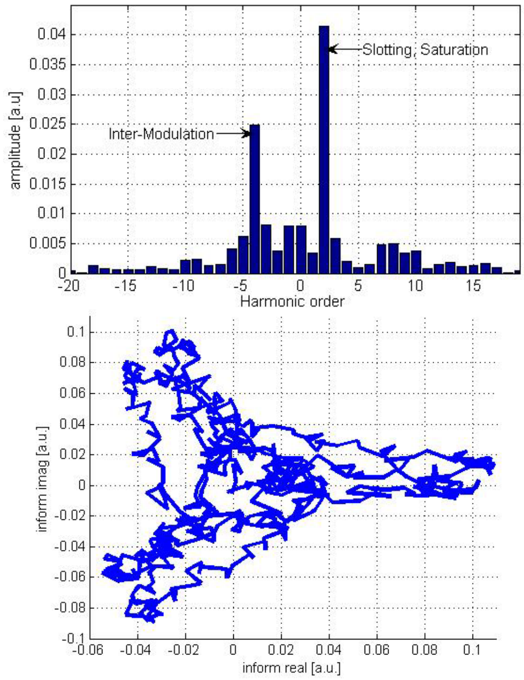

Fig. 3: Overlap of saliency signal components at 92% rated load and -2.024 rpm. Upper: FFT spectrum; Lower: XY plot of real and imaginary parts of saliency control signals.

Next speed and load current are changed to obtain another overlap situation.

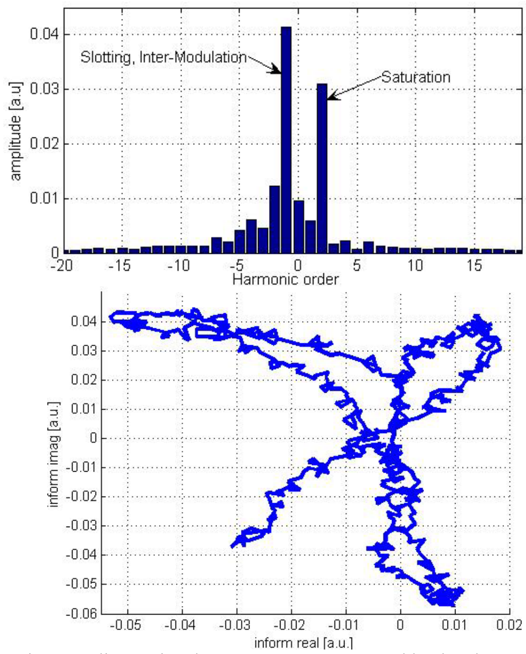

Fig. 4 : Saliency signal components at 85% rated load and 1.87 rpm. Upper: FFT spectrum; Lower: XY plot of real and imaginary parts of saliency control signals.

In Fig. 4 (upper diagram) the FFT spectrum of the resulting saliency signal at 85% rated load and the machine rotating at a speed of 1.87 rpm is depicted.

As shown in the figure at this point of operation the slotting modulation has a harmonic order of -1st. The saturation signal is visible as +2nd harmonic. Again (11) can be used to determine the harmonic component caused by the interaction of saturation and slotting signals. In this case it leads to an intermodulation component with the same order than the slotting (-1st).

The lower diagram of Fig. 4 shows the locus of the real and imaginary components of the resulting saliency control signal. At this point of operation the overlap between the slotting and the inter-modulation induced signal is clearly visible. As before an accurate feed forward separation is absolute necessary also in this point of operation.

Situation near a spectral overlap is shown in the next two figures. In Fig. 5 the machine was operated at 95%rated load and a speed of -1.8rpm. The corresponding FFT spectrum is shown in the upper diagram of the figure.

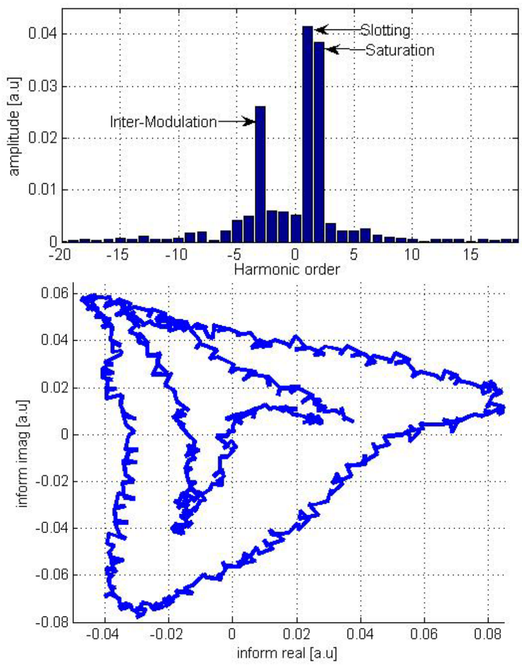

Fig. 5: Saliency signal components at 95% rated load and -1.8 rpm. Upper: FFT spectrum; Lower: XY plot of real and imaginary parts of saliency control signals.

At these operating conditions the slotting modulation is visible as +1st harmonic, and the saturation modulation as +2nd harmonic what represents operation close to a spectral overlap.

The modulation component caused by the interaction of saturation and slotting signals according to (11) is a -3rd harmonic. The corresponding locus of the real and imaginary components of the resulting saliency control signal is shown in Fig. 5 (lower diagram). Due to the beginning of the spectral overlap the real and imaginary components stop to show clear zero crossings what leads to a clear reduction in the accuracy of the extracted control angles.

Finally in Fig. 6 operation is shown with a beginning spectral overlap of saturation and inter-modulation component. The machine was operated at 90% load with a speed of 3.1 rpm. The corresponding spectrum is depicted in the upper diagram.

As can be seen in the figure at this point of operation the slotting signal corresponds to a -3rd harmonic and the saturation modulation to the +2nd harmonic. The resulting inter-modulation component according to (11) is the +1st harmonic what leads to the beginning overlap situation.

In the lower diagram of the figure the locus of the real and imaginary components of the resulting saliency control signal is shown. Though the zero crossings of the real and imaginary components are still detectable it is obvious that robustness of the extracted control angles is clearly reduced and now strongly depends on the feed forward separation of the individual saliency components.

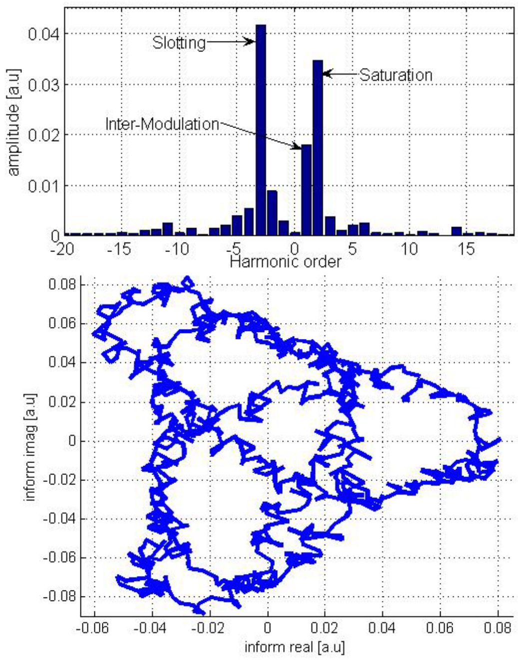

Fig. 6: Saliency signal components at 90% rated load and 3.1 rpm. Upper: FFT spectrum; Lower: XY plot of real and imaginary parts of saliency control signals.

V. Conclusion

In this paper the saliency based sensorless control methods were analyzed and a set of critical points of operation are identified that have not been addressed in literature up to now. These critical points of operation exist at any spectral overlap of the different saliency components as well as their inter-modulations. During these operating conditions a separation of the overlapping components is only possible using feed forward methods.

A mathematical description of the relation between the mechanical speed and load torque at the overlap of the different dominant harmonics caused by slotting, saturation, as well as by inter-modulation of both is presented to determine these critical points of operation.

Measurement results were presented to point out the consequences of spectral overlap on the resulting saliency signal. The saliency signal was obtained from the transient current response resulting from an excitation of the machine with a voltage pulse sequence. While the critical point of operation of fundamental wave based sensorless control is at zero frequency it can be defused when using saliency based methods. While these methods in the past only proved good performance at zero mechanical and zero electrical speed the critical overlap areas were neglected so far.

However, as was shown by the measurement results it is important to especially consider the performance at those operating states near mechanical standstill where a spectral overlap of the different signal components exists. Then the control performance strongly depends on the accuracy of the feed forward separation technique applied.

APPENDIX I

Machine parameters of the applied induction machine

Nominal Current:	30A
Nominal Voltage:	280V
Nominal Frequency:	75Hz
Rated Power:	11kW

4-poles, 36 stator teeth, un-skewed rotor, open slots, 44 rotor bars.

ACKNOWLEDGMENT

The authors gratefully acknowledge the financial support of the Austrian Science Foundation - "Fonds zur Förderung der wissenschaftlichen Forschung" (FWF) - under grant no. P19967-N14.

REFERENCES

[1] K. Rajashekara, A. Kawamura and K. Matsuse, "Sensorless Control of AC Motor Drives", IEEE Press Book, 1996.

[2] M. Schroedl, "Sensorless Control of Ac Machines at Low Speed and Standstill Based on the INFORM Method" (1996) *Proceedings of 31st IAS Annual Meeting* San Diego, Vol1, pp.270-277.

[3] J. Holtz, "Sensorless position control of induction motor-an emerging technology", Proceedings of IEEE IECON, Vol.1, pp. I1-I12, (1998).

[4] J. Ha and S. Sul, "Sensorless Field-Orientation Control of an Induction Machine by High Frequency Signal Injection", *IEEE Trans. On Ind Appl.*, Vol 35, No.1, Jan/Feb. 1999, pp. 45-51.

[5] A. Consoli, G. Scarcella, and A. Testa, "A new zero frequency flux position detection approach for direct field oriented control drives", *Proc. IEEE-IAS Annual Meeting*, Phoenix, 1999,Vol 4, pp.2290-2297.IAS, New Orleans, pp. 760-767, (1997).

[6] Q. Gao, G. M. Asher, and M. Sumner, "Sensorless Position and Speed Control of Induction Motors Using High Frequency Injection and Without Offline Precommissioning", *IEEE Trans. on Industrial Electronics*, Oct 2007, Vol. 54 pp. 2474-2481.

[7] Pablo Garcia, Fernando Briz, Dejan Racn and Robert D. Lorenz, "Saliency Tracking-based Sensorless Control of AC Machines Using Structured Neural Networks", *the 40th Annual Meeting of IEEE, IAS* 2005.

[8] T. Wolbank, J.Machl: "A modified PWM scheme in order to obtain spatial information of ac machines without mechanical sensor", Proc. *IEEE APEC*, pp.310-315, 2002, Dallas, TX.

[9] P. Weinmeier: "Sensorless high dynamic control of a hybrid reluctance machine in the low frequency range including standstill" Dissertation, Technical University of Vienna (1998)

[10] J. Holtz, J. Juliet, 'Sensorless acquisition of the rotor position angle of induction motors with arbitrary stator windings', *IEEE Industry Applications Conference,* pp.1321-1328 vol.2 (2004)

[11] Q. Gao, Asher, G.M.; Sumner, M.; Makys, P "Position Estimation of AC Machines Over a Wide Frequency Range Based on Space Vector PWM Excitation", *IEEE Trans. Ind. Appl.*, vol. 43, no. 4, pp. 1001–1011, July/Aug. 2007

[12] T. Wolbank, M.A. Vogelsberger; M. Riepler; T.G. Habetler; S. Grubic: "Integration of Transient and Fundamental Wave Excitation for Zero Speed Sensorless Control of ac Machines", Proc. *IEEE ICEM Conference*, pp.1-6, 2008, Portugal.